Adaptive Impedance Matching for Efficient Wireless Power Transmission via a Perturbance and Observation Method

1st Fatemeh Nasr Esfahani
School of Engineering
Lancaster University
Lancaster, UK
f.nasresfahani@lancaster.ac.uk

2nd Mehdi Niroomand
Dept. of Electrical Engineering
University of Isfahan
Isfahan, Iran
mehdi_niroomand@eng.ui.ac.ir

3rd Seyed M. Madani
Dept. of Electrical Engineering
University of Isfahan
Isfahan, Iran
m.madani@eng.ui.ac.ir

4th Javad Ebrahimi
Smith Engineering
Queen's University
Kingston, Canada
javad.ebrahimi@queensu.ca

5th Alireza Bakhshai
Smith Engineering
Queen's University
Kingston, Canada
alireza.bakhshai@queensu.ca

***Abstract*—Impedance mismatching is a prevalent issue in wireless power transfer (WPT) systems across various power levels and operating frequencies. In scenarios where coils are closely coupled, the maximum power transfer does not occur at the natural resonant frequency of the coupled coils due to impedance mismatching between the internal impedance of the power source and the WPT system's input impedance. This results in the frequency splitting phenomenon. This paper first examines the frequency splitting phenomenon using the maximum power transfer theorem. Subsequently, a Perturbation and Observation (P&O)-based method with a variable step size is proposed to enhance power transfer efficiency over a range of coil-to-coil distances. Unlike conventional, time-consuming search-and-find impedance matching (IM) methods, this approach achieves optimal IM network parameters in a single step. A scaled-down 20-watt prototype is fabricated to validate the effectiveness of the proposed method in terms of input current, active and reactive input powers, as well as power factor correction (PFC).**

***Index Terms*—Wireless power transfer (WPT), Inductive power transfer (IPT), Frequency splitting, Impedance matching (IM), Maximum power transfer theorem, Perturbance and Observation (P&O), Electric Vehicles (EVs)**

I. Introduction

Depending on the transmission range and operating frequency, wireless power transfer (WPT) technology is primarily categorized into three main types: Microwave Radiative Power Transfer (MRPT) for long-range [1]–[3], Magnetic Resonance Coupling (MRC) in high frequency (HF) for mid-range [4], and Inductive Power Transfer (IPT) in low frequency for short-range distances [5]. Although the efficiency of power transfer in IPT systems is relatively low over medium transmission distances compared to recently proposed mid-range WPT systems, MRC-based WPT systems encounter challenges related to electromagnetic interference (EMI), inefficient power delivery over short distances, and stabilization issues with high-Q resonators [4]–[7]. Therefore, IPT is often preferred over resonance-based systems in various applications, such as portable consumer electronics (e.g., laptops, cell phones, PDAs) [8], [9] and electric vehicles (EVs) [10]–[13]. To maintain optimal power transfer efficiency across a wide range of coil-to-coil distances, WPT systems aim to achieve critical coupling where the input impedance matches that of the power supply [1], [14], [15]. Deviation from this critical distance decreases efficiency due to phenomena like frequency splitting [4], [16], [17]. To mitigate efficiency reductions, range-adaptive control techniques are employed, particularly in scenarios of short coil-to-coil distances where impedance mismatch is significant.

Literature reports two main compensation methods: (1) frequency tracking approaches involve adaptive adjustment of the input power supply frequency based on coil-to-coil distance, constrained within the industrial, scientific, and medical (ISM) band [6], [18], and requiring additional frequency tracking circuits [19]; and (2) impedance matching (IM) techniques, including coupling manipulation through additional loops between coupled coils to narrow the distance range for effective impedance matching [15], [16], and IM methods using lossless LC circuits provide parameters through time-consuming search-and-find techniques [1], [15], while those using DC-DC converters increase system losses [20].

This paper proposes a P&O-based IM method in which the IM network parameters are extracted in a single variable step size. This method is applicable for a wide range of coil-to-coil distances and load power factors. The paper is organized as follows: In section II, the frequency splitting phenomenon is studied using the maximum power transfer theorem. In Section III, the proposed P&O-based method is presented in detail. Section IV demonstrates the experimental verification. Finally, conclusions are drawn in Section V.

II. Frequency Splitting Phenomenon

A. Two-coil WPT system circuit modeling

Fig. 1 shows the equivalent circuit of a two-coil WPT system sharing a mutual inductance M. The transmitter and receiver coils are modeled as inductors L_1 and L_2 series with their parasitic resistances R_1 and R_2, respectively. A high-frequency (HF) power supply with the internal resistance R_s is used to drive the transmitter coil and the output load R_L is assumed to be resistive here. The series capacitors C_1 and C_2 are added to resonate with L_1 and L_2 inductances, respectively, at the resonant frequency f_s [17]. The efficiency of the power transmitted η to the output load is as follows [21]:

$$\eta = \frac{P_{Load}}{P_{in}} = \frac{V_L^2/2R_L}{(V_s - R_s I_1)^2/2R_{in}} \quad (1)$$

, where V_L, V_s, and I_1 are the voltage across the output load, the amplitude of the HF power supply's voltage, and the current through the transmitter coil. Also, $R_{in} = Real(Z_{in})$ is the input resistance of the two-coil WPT system.

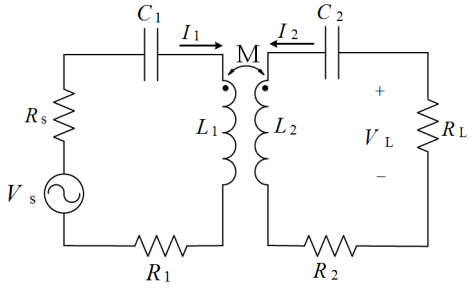

Fig. 1. Equivalent circuit of a two-coil WPT system

B. Frequency splitting analysis based on maximum power transfer theorem

In the strongly coupled region, where the coupling coefficient k deviates from the critical-coupling coefficient k_c, the efficiency η decreases. In coil-to-coil distances shorter than critical-distance d_c, there are two peaks in the efficiency curve η at the frequencies different from the coupled-coils natural resonant frequency f_s. This phenomenon is called the frequency splitting phenomenon [15], [17].

Fig. 2 shows the abstract model of a two-coil WPT system with $Z_{in} = \frac{(2\pi f_s M)^2}{R_L}$. For the system parameter values in Table I, the MATLAB simulation results for the amplitude of the WPT system input impedance $|Z_{in}|$, its phase, and the efficiency η versus normalized frequency f/f_s at the strongly coupled region with k=0.4 are shown in Fig. 3. As seen, the efficiency η peaks at splitting frequencies of about 111 kHz and 148kHz, which are known as odd f_{odd} and even f_{even} splitting frequencies, respectively [15]. At the splitting frequencies, $|Z_{in}|$ is very close to the source internal resistance R_s (here 1.2Ω). Therefore, the maximum power is transferred at these two frequencies instead of the natural resonance frequency f_s = 125kHz. In other words, as for a very short separation distance d, the coupling between coils M is large, $|Z_{in}|$ is greater than R_s, so the maximum available power is not transferred at f_s. Therefore, impedance matching is required in WPT systems with variable coil-coil distances to enable maximum wireless power transfer from the HF input power supply to the output load.

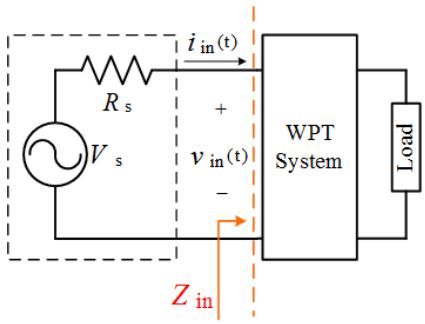

Fig. 2. Abstract model of the WPT system

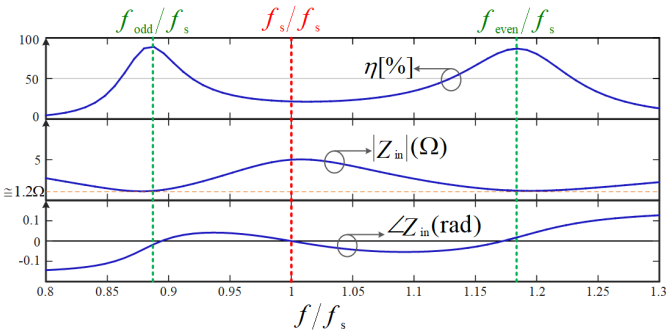

Fig. 3. Efficiency η versus normalized frequency f/f_s for different k.

TABLE I
WPT System Parameters Value

Parameter	Value	Parameter	Value
f_s	125 KHz	C_1	15.83 nF
L_1	101.4 μH	C_2	17.87 nF
L_2	15.83 nF	V_s	14.28V
R_1	0.45 Ω	R_s	1.2 Ω
R_2	0.45 Ω	R_L	10 Ω

III. The Proposed Method

A. The impedance matching network design

Smith chart is a common tool for designing IM networks [22]. The input impedance of WPT system Z_{in} can be from different types of resistive R_{in}, resistive-inductive $R_{in}+jX_{in}$, and resistive-capacitive $R_{in}-jX_{in}$. The designed IM network must be able to match all these types of impedances with the impedance of HF input power supply R_s.

Fig. 4 shows how Z_{in} is matched with R_s by adding only a parallel capacitor C_P and a series inductance L_s, regardless of its type.

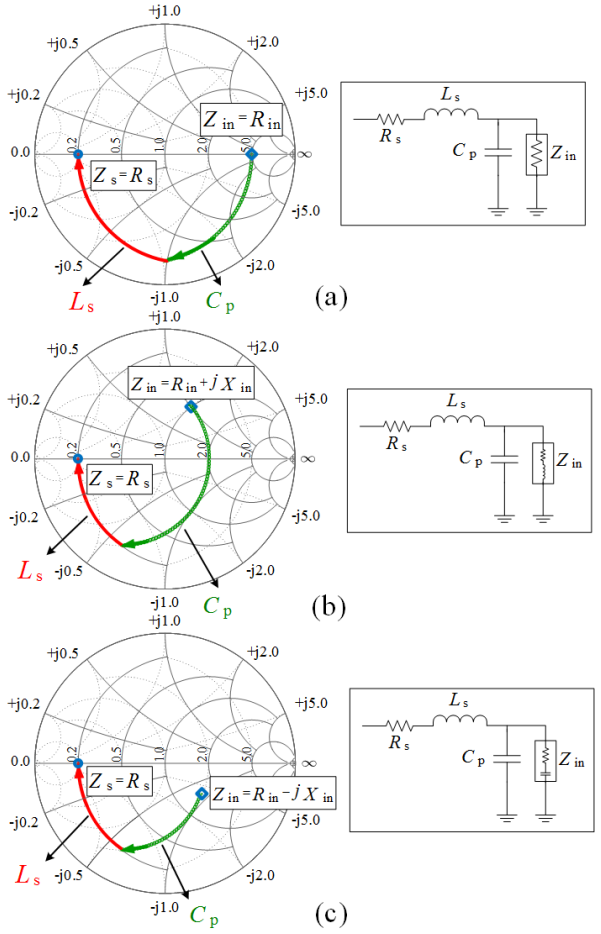

Fig. 4. IM network design for different types of the input impedance Z_{in}: (a) Resistive (R_{in}) (b) Resistive-inductive $(R_{in}+jX_{in})$ (c) Resistive-capacitive $(R_{in}-jX_{in})$

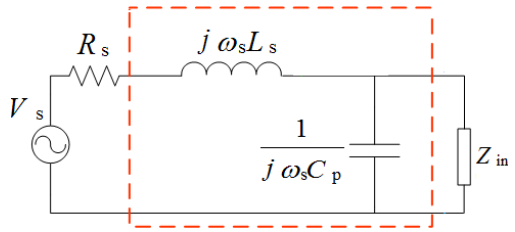

Fig. 5. Equivalent circuit of two-coil WPT system together with the designed IM network

B. IM network parameters calculation

Fig. 5 shows the equivalent circuit of the two-coil WPT system together with the designed IM network which is to match the input impedance Z_{in} with internal resistance of HF input power supply R_s as $Real(Z_{in}) = R_s$.

Quality factor (Q)-based design principles are used here to calculate the IM network parameters L_s and C_P for different types of input impedance, including Resistive (R_{in}), Resistive-inductive $(R_{in}+jX_{in})$, and Resistive-capacitive $(R_{in}-jX_{in})$.

- ***Resistive load***

For the equivalent circuit of the two-coil WPT system shown in Fig. 5, the quality factor Q is defined as:

$$Q = \frac{2\pi f_s L_s}{R_s} = 2\pi f_s C_P R_{in} \tag{2}$$

The IM network parameters can be extracted as:

$$C_P = \frac{Q}{2\pi f_s R_{in}} \tag{3}$$

$$L_s = \frac{QR_s}{2\pi f_s} \tag{4}$$

, where the quality factor Q can be calculated as:

$$Q = \sqrt{\frac{R_{in}}{R_s} - 1} \tag{5}$$

- ***Resistive-inductive load***

The quality factor Q_1 in Fig. 6 can be caculated as:

$$Q_1 = \frac{X_{in}}{R_{in}} \tag{6}$$

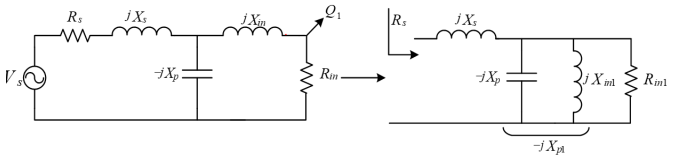

Fig. 6. Equivalent circuit of the two-coil WPT system with the IM network after series-to-parallel transformation of R_{in} and jX_{in}

After series-to-parallel transformation of R_{in} and jX_{in}, the impedances R_{in1} and jX_{in1} can be extracted as:

$$R_{in1} = R_{in}(1 + {Q_1}^2) \tag{7}$$

$$X_{in1} = \frac{X_{in}(1 + {Q_1}^2)}{{Q_1}^2} \tag{8}$$

To have an RLC circuit, the parallel combination of $-jX_p$ and jX_{in1} in Fig. 7 must serve as a capacitive impedance as:

$$-jX_p1 = (X_{in1})||(-jX_p) = \frac{(-jX_p)(X_{in}(\frac{1+{Q_1}^2}{{Q_1}^2}))}{-jX_p + X_{in}(\frac{1+{Q_1}^2}{{Q_1}^2})} \tag{9}$$

After parallel-to-series transformation of R_{in1} and $-jX_p1$, the impedances R_{in2} and X_{p2} are extracted as:

$$R_{in2} = \frac{R_{in1}}{1 + {Q_2}^2} \tag{10}$$

$$X_{p2} = X_{p1}\frac{{Q_2}^2}{1 + {Q_2}^2} \tag{11}$$

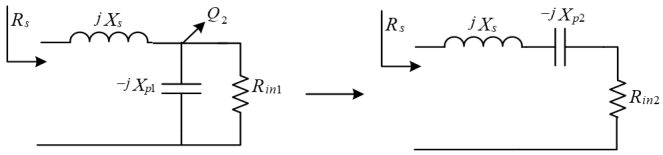

Fig. 7. Equivalent circuit of the two-coil WPT system with the IM network after parallel-to-series transformation of R_{in1} and jX_{p1}

, where Q_2 can be obtained as:

$$Q_2 = \sqrt{\frac{R_{in}(1+{Q_1}^2)}{Rs} - 1} \tag{12}$$

Finally, considering the maximum power transfer requirements as $R_{in2} = R_s$ and $X_{p2} = X_s$, the IM network parameters L_s and C_P are calculated as:

$$C_P = \frac{1}{2\pi f_s X_p} \tag{13}$$

$$L_s = \frac{Q_2 R_s}{2\pi f_s} \tag{14}$$

- ***Resistive-capacitive load***
  The IM network parameters L_s and C_P for a resistive-inductive load can be calculated using the same method and the results are:

$$C_P = \frac{1}{2\pi f_s X_p} \tag{15}$$

$$L_s = \frac{Q_3 R_s}{2\pi f_s} \tag{16}$$

, where the quality factor Q_3 in Fig. 8 is equal to:

$$Q_3 = \sqrt{\frac{{R_{in}}^2 + {X_{in}}^2}{R_{in}R_s} - 1} \tag{17}$$

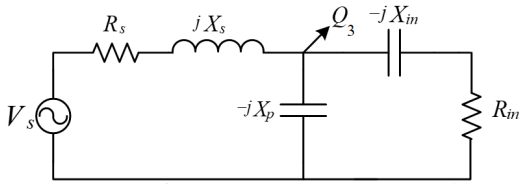

Fig. 8. Equivalent circuit of the two-coil WPT system with resistive-capacitive input impedance $R_{in} - jX_{in}$

C. The P&O based method

When the operating frequency of the WPT system is low ($Q < 10$), the Q-based method cannot provide accurate values. Inspired by the perturbance and observation (P&O) algorithm, a method is presented in this paper which can improve the power transmission efficiency of the WPT system at the strongly coupled region.

Fig. 9 shows the maximum power available from the HF input power supply for different pairs of the IM network parameters L_s and C_P. It can be seen that by starting from any point with any pairs of the IM network parameters L_s and C_P, the power curve can be moved towards the maximum power point as a result of impedance matching between Z_{in} and R_s if the right ***Rise Direction*** and proper ***Step-Size*** are chosen.

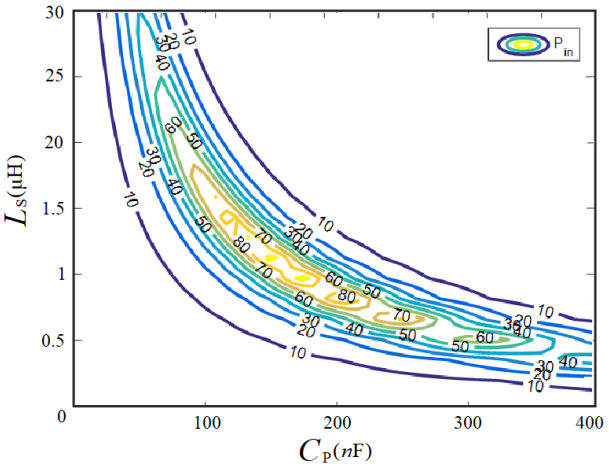

Fig. 9. Maximum power available from the HF input power supply for different pairs of the IM network parameters L_s and C_P

Algorithm 1 shows the the proposed P&O-based algorihm. Firstly a pair of IM network parameters $L_s(i)$ and $C_p(i)$ is chosen and the transferred power to the input impedance $P_{in}(i)$ is calculated. Then, each IM network parameter is changed by one step size. If at this stage the transferred power $P_{in}(i+1)$ is increased, the rise-direction is not changed and vice versa. The following equation is used to estimate the IM network parameters L_s and C_p. As can be seen, the variations in the coupling coefficient k and its sign are included in the step size.

$$X(i+1) = X(i) + (RD_X * \Delta X * (k(i+1) - k(i))) \tag{18}$$

, where RD is the rise-direction, and X represents the IM network parameters: L_s or C_p.

Algorithm 1 Proposed P&O Based Algorithm

Require: ΔC_p, RD_{C_p}, ΔL_s, RD_{L_s}
  Set: $C_p(i)$ and $L_s(i)$
  Measure: $P_{in}(i)$
  $C_p(i+1) \leftarrow C_p(i) + (RD_{C_p} \cdot \Delta C_p \cdot (k(i+1) - k(i)))$
  $L_s(i+1) \leftarrow L_s(i) + (RD_{L_s} \cdot \Delta L_s \cdot (k(i+1) - k(i)))$
  Measure: $P_{in}(i+1)$
  while true **do**
    if $P_{in}(i+1) < P_{in}(i)$ **then**
      $RD_{L_s} \leftarrow -RD_{L_s}$
      $RD_{C_p} \leftarrow -RD_{C_p}$
    end if
  end while

IV. Experimental verification

Fig. 10 shows the IM network parameters obtained from the proposed P&O-based algorithm for a step change in the coupling-coefficient k. As can be seen, the obtained values can properly track the ones calculated using eq. (3) and (4).

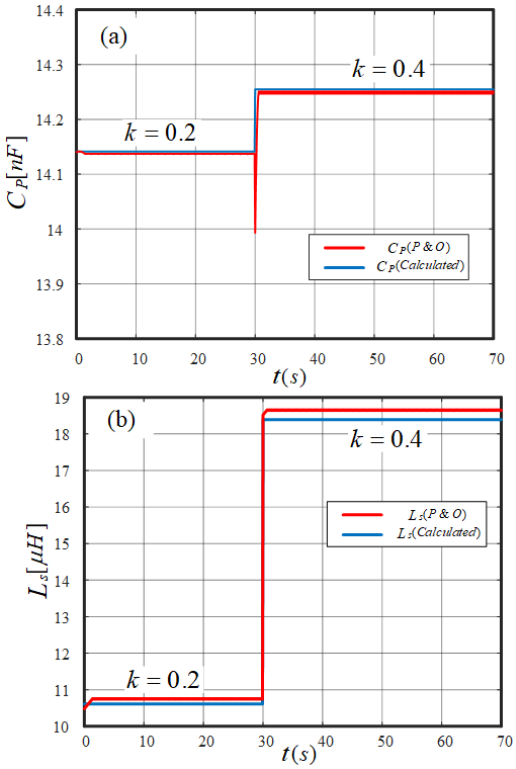

Fig. 10. Simulation results: comparison between the IM network parameters obtained using the proposed P&O-based algorithm and the calculated values (a) C_p (b) L_s

Fig. 11 shows the experimental set-up of the two-coil WPT system. The HF power supply is implemented using a function generator followed by a linear push-pull power amplifier. The variable IM network is realized using a 7-bit binary capacitor bank and a 7-bit binary inductor bank. In addition, two series capacitors resonate with the coupled coils at the frequency of the input power supply $f_s = 125kHz$.

Fig. 12 shows the input current waveforms at different coil-to-coil distances d=2, 4, and 6cm at the resonant condition. Fig. 12(a) shows that the input current has its maximum value at d=4cm which is known as critical distance d_c. At distances shorter or longer than d_c, the input current is decreased. Fig. 12(b) shows that after applying the proposed method, the input current is considerably improved for a wide range of distances from "strongly-coupled" with d=2cm to "weakly-coupled" with d=6cm.

After applying the proposed IM method, the input active power P_{in} shown in Fig. 13(a) is also increased from less than 5 watts to around 20W. Additionally, Fig. 13(b) shows that the input reactive power Q_{in} is considerably decreased as a result of the power factor correction at the input of the WPT system.

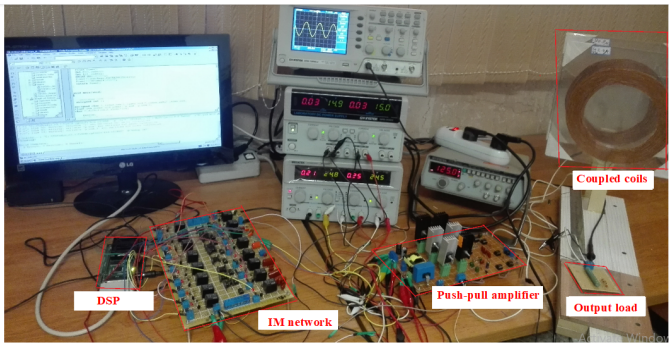

Fig. 11. Experimental setup of the proposed IM method

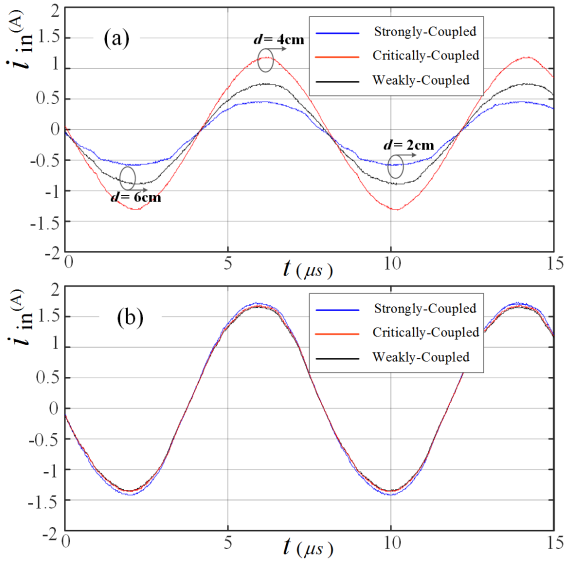

Fig. 12. Experimental results for input current at different distances (a) before applying the proposed method (b) after applying the proposed method

V. Conclusion

In this paper, a P&O-based method with a variable step size was introduced to enhance power transfer capability in the strongly coupled region of a two-coil WPT system. The IM network parameters obtained using this method accurately track the calculated values due to the appropriate rise direction and step size. Experimental results confirm the effectiveness of the proposed P&O-based method in improving input current, active input power, and PFC. Given an operating frequency of f_s=125kHz, the P&O-based method is well-suited for wireless charging of EVs across varying coil-to-coil distances.

References

[1] A. P. Sample, D. T. Meyer, and J. R. Smith,"Analysis, experimental results, and range adaptation of magnetically coupled resonators for wireless power transfer,"IEEE Trans. Ind. Electron., vol. 58, no. 2, pp. 544-554, Feb. 2011.

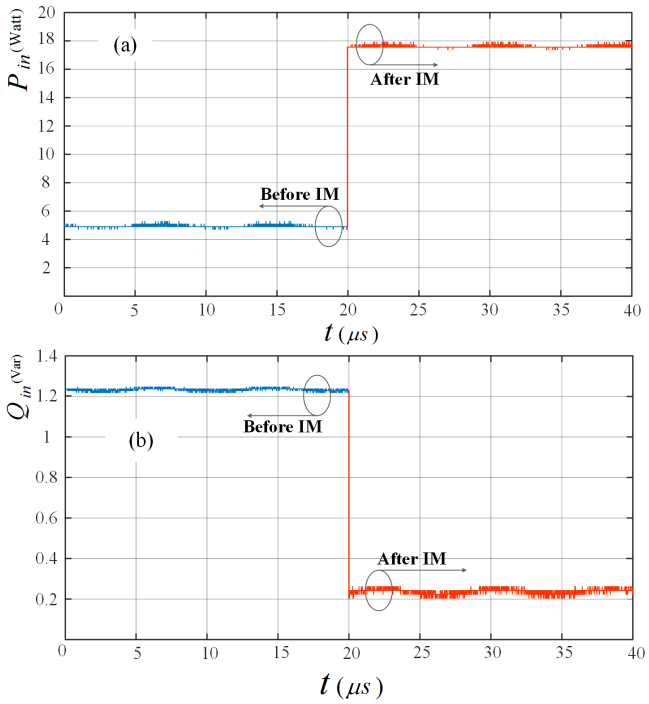

Fig. 13. Experimental results illustrating the effect of impedance matching on the average values of: (a) input active power P_{in} (b) input reactive powers Q_{in}

[2] H. Zhou, Z. Shen, Y. Wu, Y. Zhuang, and Y. Zhang, "An Anti-Misalignment Wireless Charging System for Low-Power Applications Based on Solenoid Coils Incorporated With Reverse Windings," *IEEE Transactions on Consumer Electronics*, vol. 70, no. 1, pp. 371-377, Feb. 2024.

[3] M. Rehman, et al., "A Review of Inductive Power Transfer: Emphasis on Performance Parameters, Compensation Topologies and Coil Design Aspects," *IEEE Access*, vol. 11, pp. 144978-145010, 2023.

[4] J. Lee, Y. S. Lim, W. J. Yang, and S. O. Lim,"Wireless power transfer system adaptive to change in coil separation,"IEEE Trans. Antennas Propag., vol. 62, no. 2, pp. 889-897, 2014.

[5] J. Kim, and J. Jeong,"Range-adaptive wireless power transfer using multiloop and tunable matching techniques,"IEEE Trans. Ind. Electron., vol. 62, no. 10, pp. 6233-6241, 2015.

[6] W. S. Lee, W. I. Son, K. S. Oh, and J. W. Yu,"Contactless energy transfer systems using antiparallel resonant loops,"IEEE Trans. Ind. Electron., vol. 60, no. 1, pp. 350-359, 2013.

[7] W. Li, F. Yu, X. Rong and H. Qin, "Optimization of Low-Frequency Magnetic Metamaterials for Efficiency Improvement in Magnetically Coupled Resonant Wireless Power Transfer Systems," *IEEE Access*, vol. 10, pp. 125445-125457, 2022.

[8] C. Duan, C. Jiang, A. Taylor, and K. H. Bai,"Design of a zero-voltage-switching large-air-gap wireless charger with low electric stress for electric vehicles,"IET Power Electron., vol. 6, no. 9, pp. 1742-1750, 2013.

[9] Y. Zhang, S. Chen, X. Li, and Y. Tang, "Design Methodology of Free-Positioning Nonoverlapping Wireless Charging for Consumer Electronics Based on Antiparallel Windings," *IEEE Transactions on Industrial Electronics*, vol. 69, no. 1, pp. 825-834, Jan. 2022.

[10] M. Kim, D. Joo, and B. K. Lee,"Design and control of inductive power transfer system for electric vehicles considering wide variation of output voltage and coupling coefficient,"IEEE Trans. Power Electron., vol. 34, no. 2, pp. 1197-1208, Feb. 2019.

[11] Y. Chen, et al., "A Clamp Circuit-Based Inductive Power Transfer System With Reconfigurable Rectifier Tolerating Extensive Coupling Variations," *IEEE Transactions on Power Electronics*, vol. 39, no. 2, pp. 1942-1946, Feb. 2024.

[12] M. Vinod, D. Kishan, and B. D. Reddy, "Three-Leg DC-DC Converter for Efficient Inductive Power Transfer of Electric Vehicles for Wide-Range Battery Applications," *IEEE Transactions on Power Electronics*, vol. 38, no. 8, pp. 9317-9321, Aug. 2023.

[13] F. Nasr Esfahani, A. Darwish, X. Ma, and P. Twigg, "Non-Integrated and Integrated On-Board Battery Chargers (iOBCs) for Electric Vehicles (EVs): A Critical Review," *Energies*, vol. 17, no. 10, pp. 2285, 2024, doi: 10.3390/en17102285.

[14] T. C. Beh, M. Kato, T. Imura, S. Oh, and Y. Hori,"Automated impedance matching system for robust wireless power transfer via magnetic resonance coupling,"IEEE Trans. Ind. Electron., vol. 60, no. 9, pp. 3689-3698, 2013.

[15] W.Q. Niu, Chu, X. J., W. Gu, and A.D. Shen,"Exact analysis of frequency splitting phenomena of contactless power transfer systems,"IEEE Trans. Circuits Syst. I, vol. 60, no. 6, pp. 1670-1677, 2013.

[16] Y. Lyu et al.,"A method of using nonidentical resonant coils for frequency splitting elimination in wireless power transfer,"IEEE Trans. Power Electron., vol. 30, no. 11, pp. 6097-6107, Nov. 2015.

[17] F. Nasr, M. Madani, and M. Niroomand,"Precise analysis of frequency splitting phenomenon of magnetically coupled wireless power transfer system,"IEEE Asia Pac. Microw. Conf. (APMC), pp. 219-224, Nov. 2017.

[18] F. Nasr, S. M. Madani, and M. Niroomand,"Dual-objective control strategy for maximum power and efficiency point tracking in wirelessly powered biomedical implanted devices,"IET Microw. Antennas Propag., vol. 14, no. 1, pp. 36-44, 2019.

[19] P. Chen, H. Yang, R. Luo and B. Zhao,"A tissue-channel transcutaneous power transfer technique for implantable devices,"IEEE Trans. Power Electron., vol. 33, no. 11, pp. 9753-9761, Nov. 2018.

[20] Y. Huang, N. Shinohara, and T. Mitani,"Impedance matching in wireless power transfer,"IEEE Trans. Microw. Theory Tech., vol. 65, no. 2, pp. 582-590, Feb. 2017.

[21] F. N. Esfahani, S. M. Madani, M. Niroomand, and A. Safaee, "Maximum Wireless Power Transmission Using Real-Time Single Iteration Adaptive Impedance Matching," in *IEEE Transactions on Circuits and Systems I: Regular Papers*, vol. 70, no. 9, pp. 3806-3817, Sept. 2023.

[22] Y. Shao, H. Zhang, M. Liu, and C. Ma, "Explicit Design of Impedance Matching Networks for Robust MHz WPT Systems With Different Features," *IEEE Transactions on Power Electronics*, vol. 37, no. 9, pp. 11382-11393, Sept. 2022.